Cis → *Trans* Photoisomerisation of Azobenzene: a Fresh Theoretical Look ESI

Isabella C.D. Merritt, Denis Jacquemin, and Morgane Vacher*

Laboratoire CEISAM - UMR 6230 - CNRS - Université de Nantes, Nantes, France.

Contents

1 Orbital descriptions

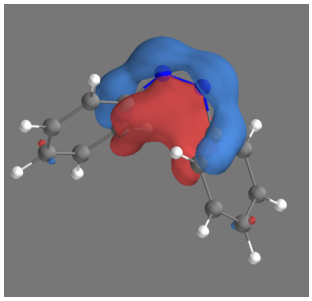	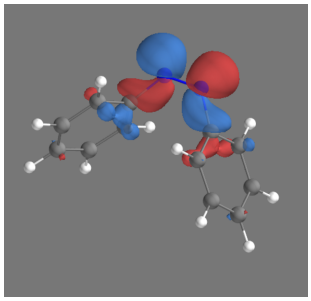	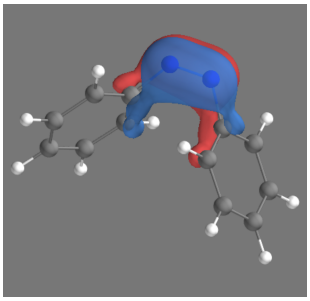	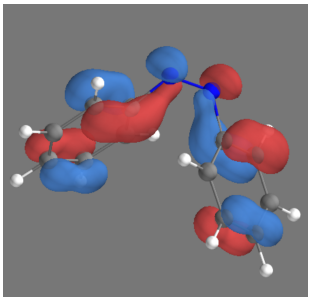
n^-	n^+	π	π
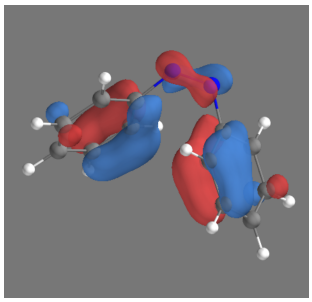	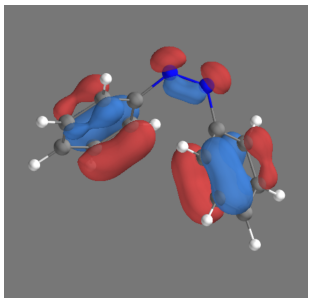	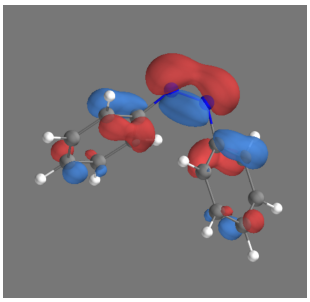	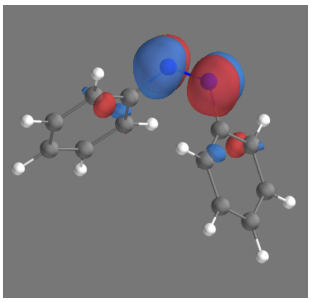
π	π	π	π^*
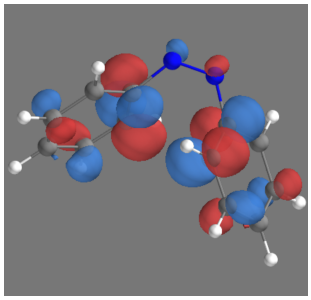	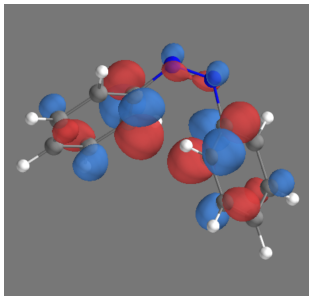	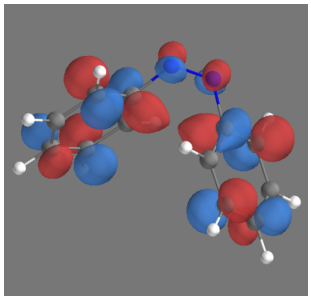	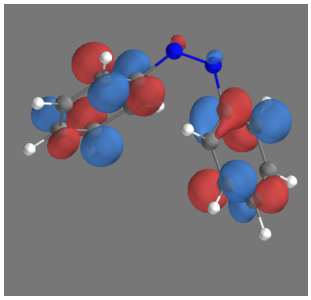
π^*	π^*	π^*	π^*

Table S1: Orbitals included in active space.

2 Optimised Geometries

Cartesian coordinates of the optimised geometries are given below, in Å. Optimisations have been carried out at the SA4-CASSCF(14,12)/ANO-RCC-VDZP level of theory.

2.1 *Cis*-Azobenzene

C	-3.23505374	0.50865244	2.17982793
C	-3.38608074	0.50998470	0.79629079
C	-4.60512617	0.84788107	0.22648326
C	-5.65859552	1.24760026	1.04068590
C	-5.51120734	1.26737699	2.40940598
C	-4.30308203	0.88741231	2.98277062
N	-2.36286806	0.01531585	-0.08149070
N	-1.25056263	0.55677613	-0.17723352
C	-0.91805049	1.75915411	0.53328058
C	0.16862481	1.70707329	1.40168895
C	0.58810026	2.86263736	2.04593641
C	-0.04863067	4.06894227	1.79594873
C	-1.09648456	4.12228727	0.90419448
C	-1.54228061	2.96616855	0.26586157
H	-6.59565377	1.52811064	0.59458930
H	-4.72426905	0.79784775	-0.84037319
H	-2.30324891	0.21340196	2.62303482
H	-4.18936922	0.88796766	4.05137836
H	-6.33217699	1.56530481	3.03596896
H	0.67290476	0.77187822	1.56399474
H	-2.35807238	3.01321507	-0.43000249
H	1.41592325	2.82051800	2.73011759
H	-1.58052886	5.05932433	0.69645991
H	0.28408968	4.96433395	2.28889101

Table S2: Optimised Geometry for Cis-AZB.

2.2 *Trans*-Azobenzene

C	-4.97736572	0.43606905	-2.43720991
C	-3.61790713	0.41432886	-2.16919219
C	-3.18045563	0.46554623	-0.84032754
C	-4.10519925	0.53731757	0.19229214
C	-5.46774185	0.55842476	-0.09166585
C	-5.90184008	0.50838990	-1.39417978
H	-5.32008114	0.39717422	-3.45521691
H	-2.90274998	0.35890790	-2.96508147
H	-3.75211458	0.57591684	1.20590561
H	-6.17816990	0.61409475	0.71319821
H	-6.95434051	0.52458502	-1.61312042
N	-1.81611382	0.44977281	-0.44122724
N	-0.99685610	0.38575061	-1.36441085
C	0.36748748	0.37004431	-0.96531414
C	1.29222971	0.29825144	-1.99793303
C	0.80494219	0.42136880	0.36354563
C	2.65477260	0.27709832	-1.71397289
H	0.93913899	0.25942011	-3.01153549
C	2.16440271	0.39971193	0.63155857
H	0.08978779	0.47688814	1.15943052
C	3.08887504	0.32732887	-0.41146834
H	3.36520608	0.22165480	-2.51884780
H	2.50711641	0.43852485	1.64956927
H	4.14137474	0.31110491	-0.19252609

Table S3: Optimised Geometry for Trans-AZB.

2.3 S_1/S_0 optimised CI

C	-0.60389945	1.96803170	0.80583128
C	-0.04117312	1.65639083	-0.44318453
C	0.88996341	2.53757698	-1.02021576
C	1.24583009	3.68529705	-0.36071300
C	0.69468279	4.00684120	0.87651155
C	-0.23203021	3.14179300	1.44804262
N	-0.38451671	0.52542694	-1.09828237
N	-1.15200619	-0.46145679	-1.02650342
C	-0.67354529	-1.63523418	-0.42005304
C	-1.56710265	-2.70815628	-0.38602787
C	-1.20172307	-3.89232021	0.21388830
C	0.05757494	-4.03150232	0.77596292
C	0.95954619	-2.96980767	0.73441860
C	0.60228907	-1.76992950	0.13704282
H	1.96117967	4.34799858	-0.81445135
H	1.31213255	2.29922881	-1.97870080
H	-1.31963192	1.30159349	1.24880173
H	-0.67085459	3.37676622	2.40123071
H	0.97944730	4.91150410	1.38044032
H	-2.53683996	-2.58544505	-0.83104827
H	1.29718556	-0.95390307	0.09496173
H	-1.89606164	-4.71240043	0.24243160
H	1.93823834	-3.07955619	1.16476465
H	0.34131489	-4.95873722	1.23932230

Table S4: Optimised Geometry for S_1/S_0 CI (C−N=N−C=−93.1).

2.4 S_2/S_1 optimised CI

C	0.765173	1.952115	1.358652
C	0.769320	1.085488	0.231658
C	-0.028977	1.437914	-0.915974
C	-0.769423	2.677447	-0.892024
C	-0.751155	3.460180	0.190863
C	0.022163	3.097667	1.360288
H	1.367891	1.694745	2.210645
H	1.507790	0.315909	0.157615
H	-1.348145	2.927501	-1.761687
H	-1.318229	4.373487	0.205666
H	0.018912	3.747501	2.215587
N	-0.274410	0.597419	-1.913124
N	0.274218	-0.597396	-1.913147
C	0.028873	-1.437970	-0.916064
C	0.769273	-2.677542	-0.892141
C	-0.769347	-1.085494	0.231640
C	0.751265	-3.460113	0.190860
H	1.347815	-2.927721	-1.761890
C	-0.764997	-1.952023	1.358716
H	-1.508136	-0.316232	0.157427
C	-0.021874	-3.097489	1.360401
H	1.318430	-4.373362	0.205701
H	-1.367848	-1.694755	2.210648
H	-0.018580	-3.747277	2.215737

Table S5: Optimised Geometry for S_2/S_1 CI (C−N=N−C=−59.9).

3 Basis set testing

To test the dependence of state energies on the chosen basis set, single point SA6-CASSCF(14,12) energy calculations were carried out on the *cis* optimised geometry using ANO-RCC-VDZP and ANO-RCC-VTZP basis sets.

"State"	VDZP Energy (eV)	VTZP Energy (eV)
S0	0.000	0.000
S1	3.476	3.479
S2	5.530	5.522
S3	6.051	6.046
S4	6.131	6.130
S5	6.439	6.424

Table S6: Energies of 6SA-CASSCF(14,12)/ANO-RCC-VDZP versus 6SA-CASSCF(14,12)/ANO-RCC-VTZP.

4 CASSCF vs CASPT2

Single point MS-CASPT2 energy calculations were carried out on both isomers to check for changes in the ordering of states on the inclusion of dynamic correlation. The state ordering of the first 4 states for *cis*-AZB was the same at both CASSCF and CASPT2 levels, while there was reordering of the S_2-S_5 states for optimised *trans*-AZB. However, since this

state reordering was only observed at the fully C_{2h} symmetric *trans*-AZB ground state, it was concluded that CASSCF can be used for the *cis* $\rightarrow$ *trans* photo-isomerisation without significant issue, as it is assumed that the molecule will no longer be in the S_2 state by the time it reaches the *trans* geometry.

Description of Dominant CI Configuration	CASSCF Energy (E_h)	Relative CASSCF Energy (eV)	MS-CASPT2 Energy (E_h)	Relative MS-CASPT2 Energy (eV)
Ground State	-569.59623	0.000	-571.42345	0.000
$n^+ \rightarrow \pi_1^*$	-569.46817	3.483	-571.32585	2.655
$\pi^5 \rightarrow \pi_1^*$	-569.38949	5.623	-571.25874	4.480
$\pi^3 \rightarrow \pi_1^*$	-569.37252	6.085	-571.25362	4.619
$\pi^2 \rightarrow \pi_1^*$	-569.35599	6.535	-571.25283	4.641
$\pi^4 \rightarrow \pi_1^*$	-569.36995	6.155	-571.24653	4.812

Table S7: Energies and definitions of the first 6 states at CASSCF and CASPT2 levels of theory, for Cis-Azobenzene (Z-AZB).

Description of Dominant CI Configuration	CASSCF Energy (E_h)	Relative CASSCF Energy (eV)	MS-CASPT2 Energy (E_h)	Relative MS-CASPT2 Energy (eV)
Ground State	-569.62208	0.000	-571.44351	0.000
$n^+ \rightarrow \pi_1^*$	-569.50234	3.257	-571.35200	2.489
$\pi^5 \rightarrow \pi_1^*$	-569.39047	6.300	-571.30875	3.665
$\pi^3 \rightarrow \pi_1^*$	-569.41324	5.680	-571.28259	4.377
$\pi^5+ \rightarrow \pi_2^*$	-569.39601	6.149	-571.27190	4.668
$\pi^4 \rightarrow \pi_1^*$	-569.41341	5.676	-571.26870	4.755

Table S8: Energies and definitions of the first 6 states at CASSCF and CASPT2 levels of theory, for Trans-Azobenzene (E-AZB).

We also compared the SA4-CASSCF (used in this work) to MS-CASPT2 energies along the central torsional coordinate, as shown in Figure S1: the CASSCF method chosen can qualitatively reproduce the shapes of the potential energy surfaces, in particular around the Franck-Condon region and around -90° where the lowest three states are close in energy and coupling vectors (and thus surface hopping probabilities) are expected to be high. As a result, we expect the surfaces used in this work to give qualitatively correct dynamics.

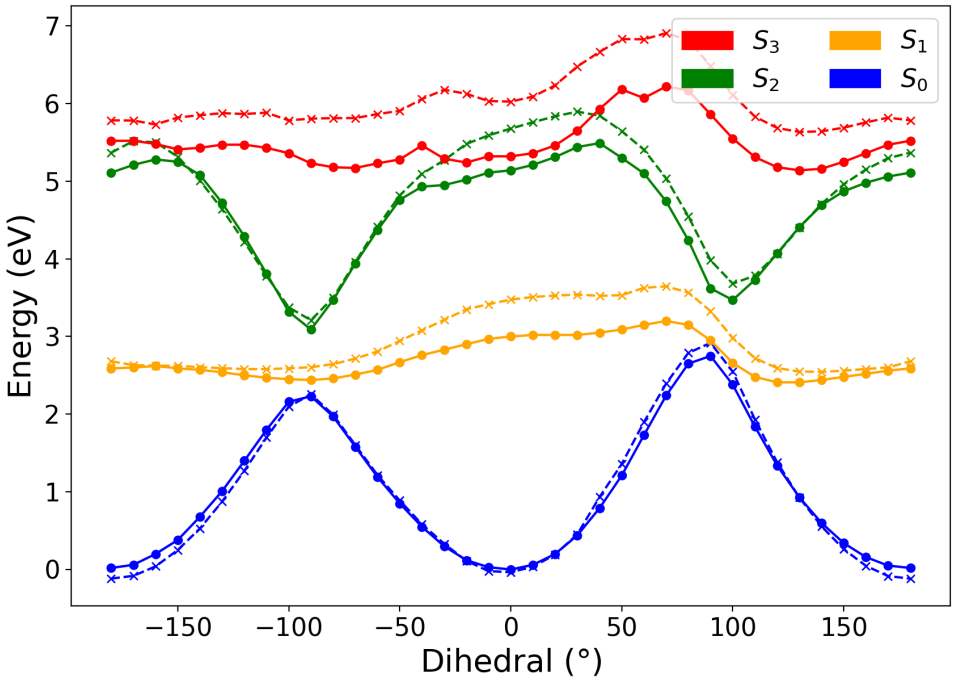

Figure S1: Comparison of a rigid scan of the first 4 electronic states along the central C−N=N−C torsional coordinate at the SA4-CASSCF(12,14)/ANO-RCC-VDZP (dashed line) and MS-CASPT2(12,14)/ANO-RCC-VDZP (solid line) levels of theory

5 Definition of Clockwise and Anticlockwise rotation

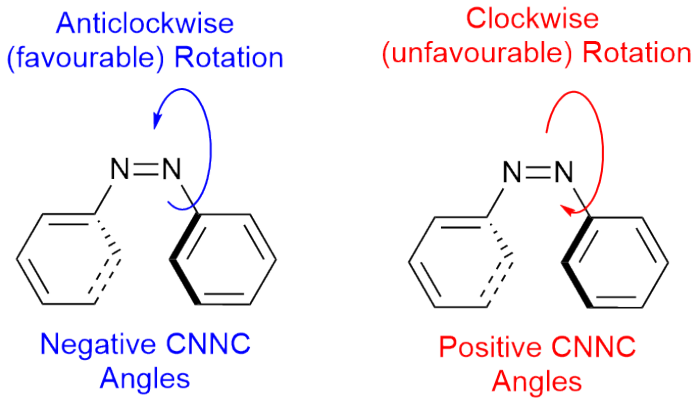

Figure S2: Definition of the favourable anti-clockwise direction (negative dihedral angles) and unfavourable clockwise direction (positive dihedral angles) starting from Cis-AZB

6 Rigid CNNC Torsion Scans

A rigid scan along the central C−N=N−C coordinate (the primary coordinate in the photo-isomerisation mechanism [1,2]) was carried out to confirm that 4 states in the state average is sufficient when describing the rotational mechanism.

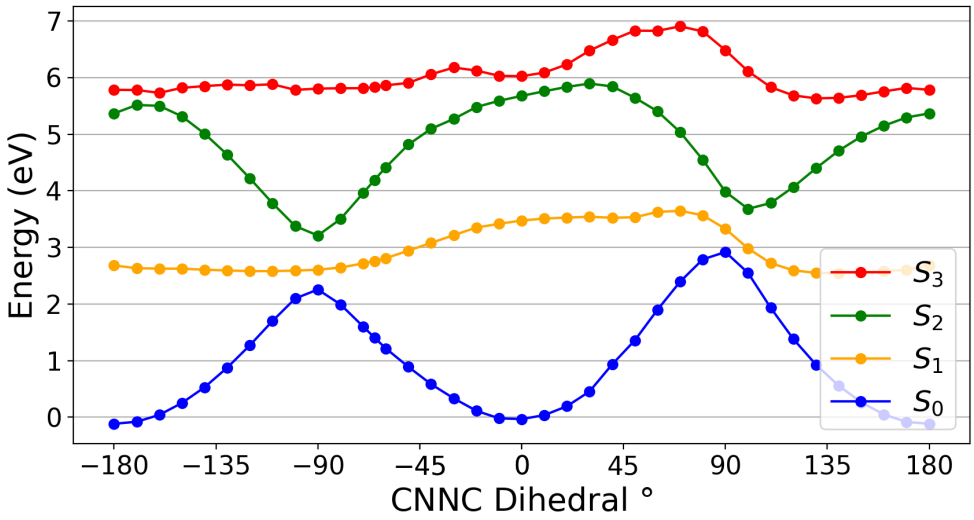

Figure S3: Rigid scan of potential energy of the first 4 electronic states along the central C−N=N−C torsional coordinate, at the SA4-CASSCF(12,14)/ANO-RCC-VDZP level of theory.

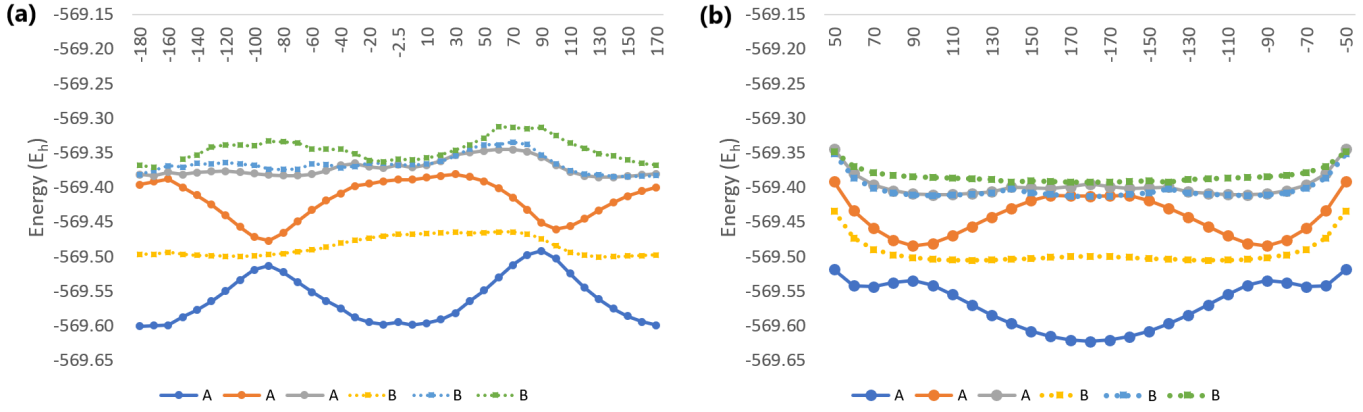

Figure S4: Rigid scans of potential energy of the first 3 electronic states of each symmetry (A and B) along the central C−N=N−C torsional coordinate, starting from **(a)** - *cis*-azobenzene and **(b)** - *trans*-azobenzene.

7 Trajectory Convergence

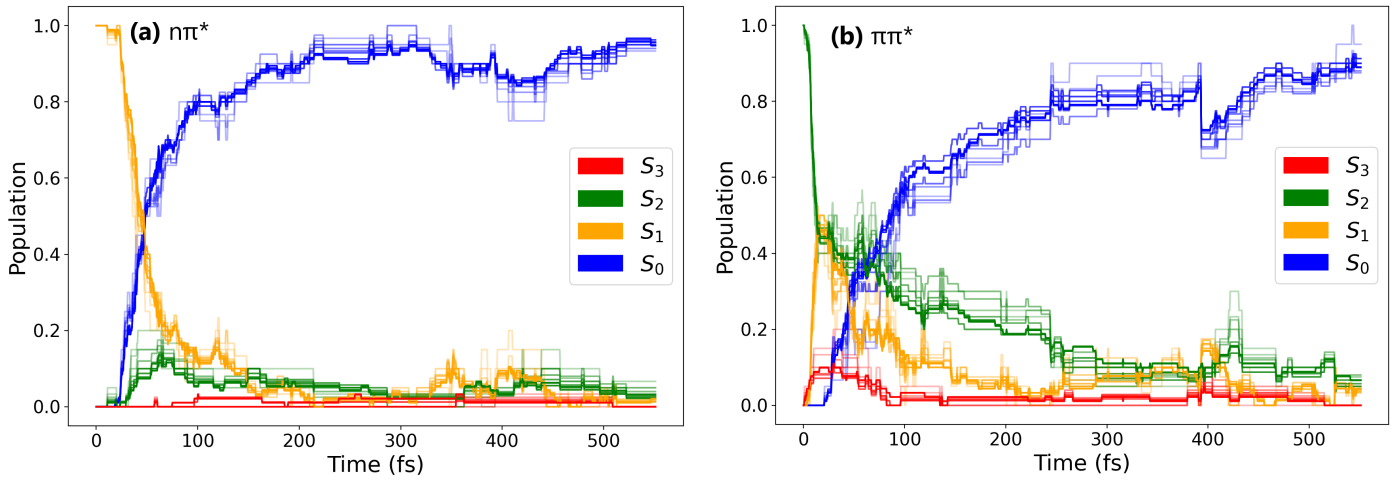

Figure S5: Convergence of simulations with increasing number of trajectories. Ensemble size starting from 10 trajectories and increasing in steps of 10, with lighter lines corresponding to fewer trajectories in the ensemble.

8 Timestep Energy Conservation

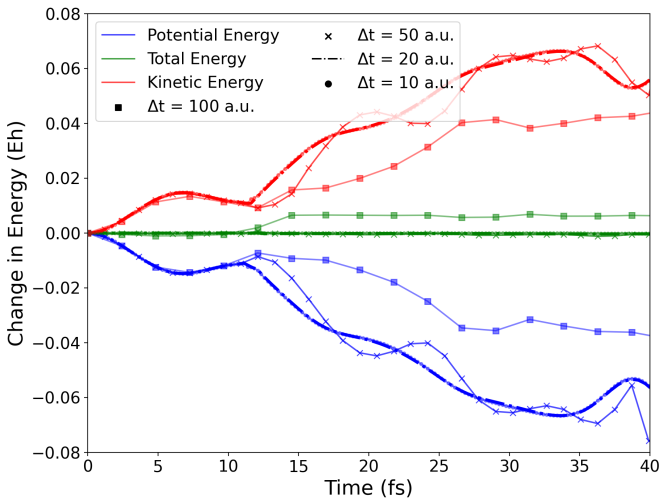

Figure S6: Potential energy, total energy, and kinetic energy obtained with different timesteps: 100 a.u., 50 a.u., 20 a.u., and 10 a.u. This is for the "unsampled" trajectory (initiated at the equilibrium geometry of the electronic ground state without kinetic energy).

9 Dynamics Analysis

9.1 Electronic populations

The population of the S_1 state for the full ensemble of trajectories after $n\pi^*$ excitation is shown in blue, while the population of the S_1 state for the $\pi\pi^*$ excitation trajectories that undergo rapid $S_2 \rightarrow S_1$ transfer is shown in red - the two decays match almost perfectly.

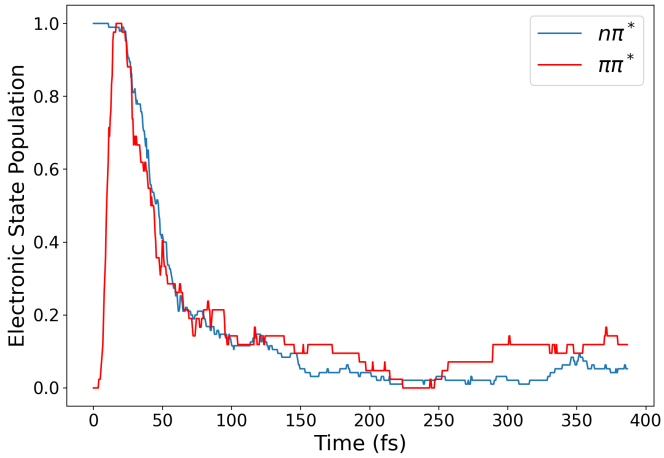

Figure S7: Comparing the evolution of S_1 population after $n\pi^*$ excitation (blue) and after $\pi\pi^*$ excitation followed by rapid (within 20 fs) $S_2 \rightarrow S_1$ decay (red).

9.2 Internal coordinates

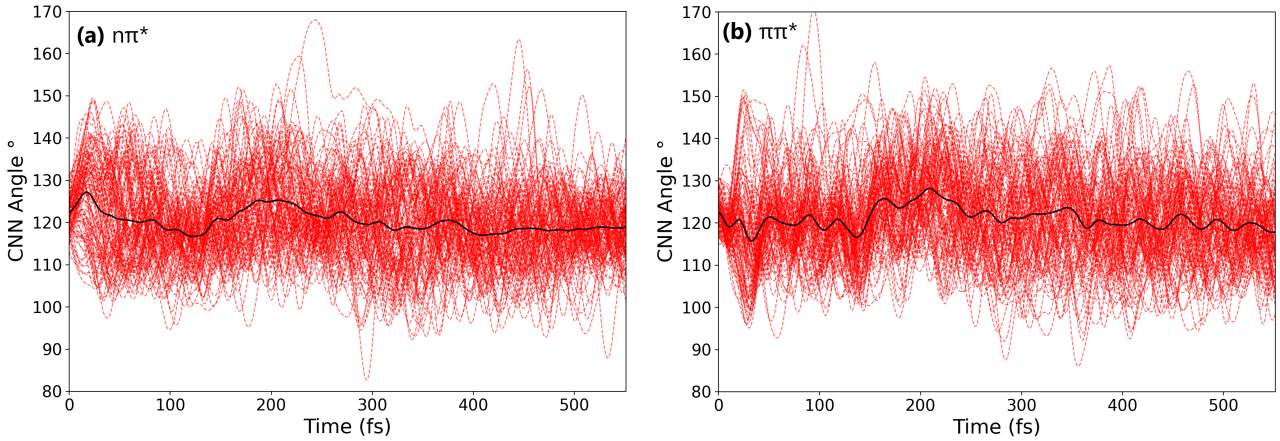

Figure S8: Evolution of the C−N=N angle after excitation to the **(a)** $n\pi^*$ and **(b)** $\pi\pi^*$ states.

9.3 Trajectory assignment

Figures S9**(a)** and S9**(b)** show the change in average potential energy through the simulations, for the S_1 and S_2 excitations respectively. The difference between reactive and non-reactive trajectories is clear. For the first 100 fs, reactive and non-reactive are relatively indistinguishable, but after this the reactive trajectories are lower in energy than the non-reactive. The apparent recovery of degeneracy at around 420 fs (most notable for $n\pi^*$ excitation) is due to the C−N=N−C rotation continuing past the isomer values (0° or 180°) as can be seen in Figures 3**(a)** and **(b)**, before rotating back towards the final isomer values. This is most notable for the *trans*-AZB pathway, where the rotation continues past 180°, reaching around 230° at around 400 fs.

Since *trans*-AZB is the thermodynamically favoured isomer (0.7 eV lower in energy at the level of theory used in this study), the fact that the reactive trajectories are around this value lower than non-reactive indicates that these trajectories have in fact isomerised, confirming that the method used to assign reactive trajectories is valid. Since the

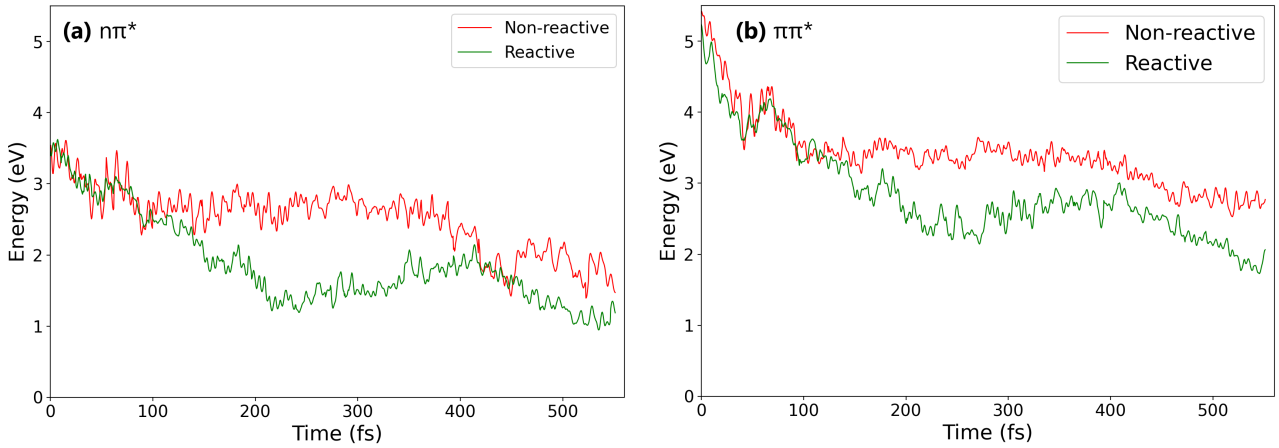

Figure S9: Average potential energy throughout the simulation for reactive (*trans*-AZB forming) trajectories vs non-reactive (*cis*-AZB forming) trajectories after $n\pi^*$ **(a)** and $\pi\pi^*$ **(b)** excitation. The average of the trajectories our method assigns as reactive (forming *trans*-AZB) are shown in green, and non-reactive (forming *cis*-AZB) in red.

reactive trajectories are clearly lower in energy after the first 200 fs, we can also conclude that although isomerisation may be complete, the fate of the photochromes is essentially "decided" within the first 200 fs.

9.4 Characterisation of hopping geometries

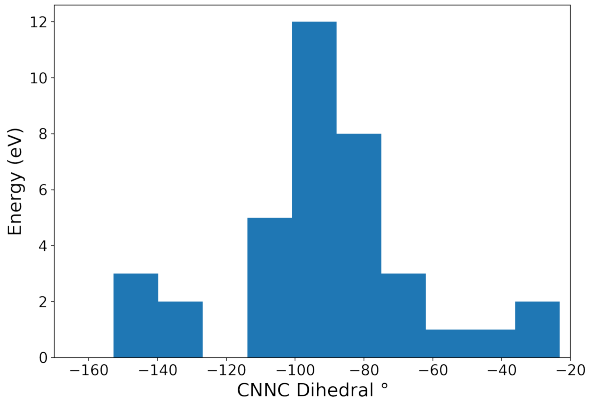

Figure S10: Distribution of dihedral angles at S_2/S_1 hopping geometries leaving the S_2 potential well.

References

[1] I. Conti, M. Garavelli and G. Orlandi, *J. Am. Chem. Soc.*, 2008, **130**, 5216–5230.

[2] Y. Ootani, K. Satoh, A. Nakayama, T. Noro and T. Taketsugu, *J. Chem. Phys.*, 2009, **131**, 194306.